TIR-LIF: A Validation Tool for Spray Impact Models

M. Alonso*[,1], P.J. Kay[1], P.J. Bowen[1], R. Gilchrist[2] and S. Sapsford[2]
[1] Cardiff School of Engineering, The Parade, Cardiff, CF24 3AA, UK
[2] Ricardo UK, Shoreham Technical Centre, Shoreham-by-sea, BN43 5FG, UK

Abstract

An experimental study of spray impact onto flat rigid surfaces is presented and discussed in this paper, which describes the use of Total Internal Reflection Laser Induced Fluorescence (TIR-LIF) as a tool for characterisation of fuel films, providing input data for validation of empirical models. In order to describe the spray/wall interaction process accurately, it is crucial to determine two interacting characteristics: i) the generation of secondary droplets, and ii) the accumulation of a liquid fuel film on the wall. Extensive research has been undertaken to characterise the post-impingement spray using Phase Doppler Anemometry (PDA). Although this technique offers considerable potential for quantification of post-impact droplet sizes and flowfield, a full understanding of the impingement process requires quantification of the mass and the spatial distribution of any residual fuel film. Hence, time-resolved spatial field measurements of droplet size need to be complemented by characterisation the resulting liquid fuel film on the wall. This paper describes the use of the TIR-LIF technique, proposed by Alonso et al [1], for characterisation of transient liquid fuel films formed as a result of spray impingement of a gasoline DI spray on a flat surface under atmospheric and elevated ambient pressures. The TIR-LIF technique is an extension of LIF in which the propagation of a laser beam is carefully controlled so as to target the excitation of the liquid fuel film only and not the airborne droplets above the film. The technique is based on the principle that upon excitation by laser light, the intensity of the fluorescent signal from a tracer is proportional to the film thickness. A frequency quadrupled Nd:YAG laser at wavelength 266 nm is used as the excitation light source and an intensified CCD camera records the results as florescent images. A binary mixture of 10 % 3-Pentanone in Isooctane is used as a substitute of gasoline due to its similar thermofluid properties. Calibrated results presented in this paper demonstrate the ability of this technique for spatial and temporal characterisation of fuel films throughout the injection event. Quantitative results reported include time resolved distribution maps of fuel film thickness, transient average film thickness, aggregate mass deposits, and film footprint area. Observations of the transient development of the 3D liquid fuel films include details of fine surface waves. This information, in conjunction with post-impingement PDA characterisation, can be used for development of post-impingement empirical models and furthermore, for appraisal of integrated Computational Fluid Dynamics (CFD) predictions of spray impingement.

Introduction

Extensive research has been undertaken over the past couple of decades to formulate and validate numerical models to describe the spray impact phenomenon (see [2] for a review). A number of spray impact models have been proposed in the literature, the most popular being the Bai and Grossman [3], Mundo et al [4], and the Stanton and Rutland model [5]. The formulation of spray impact models is generally based on experiments of single droplets impacting normally onto dry or wet walls, where the impact conditions are carefully controlled. Results from single droplets impact are then extrapolated to multiple droplet impact (spray impact) by simple superimposition of multiple individual droplets. However, such simplification neglects to consider various effects of the spray impact process such as: the influence of the deposited film on the post-impact spray, the tangential momentum of oblique impacting droplets, the effect of multiple droplets interaction, the effect of film fluctuations on the outcome of impacting droplets, and the creation of secondary droplets due to break up of the liquid film [6]. In fact, the literature shows that a single drop impact differs from the impact of a train of drops on a stationary film [7]. Also, observations by Sivakumar and Tropea [8] show that the impact resulting from a single drop differs significantly from the impact resulting from a drop within a spray. Therefore, the development of new empirical spray impact models often involve the analysis of more challenging experimental configurations involving the interaction of multiple drops [e.g. 6].

In order to describe accurately the spray impact phenomenon, it is crucial to determine correctly two interacting characteristics: *i*) the generation of secondary droplets, and *ii*) the accumulation of a liquid fuel film on the wall. The relative interaction of these characteristics is influenced greatly by pre-impact conditions, such as: ambient condi-

*Corresponding author: AlonsoM@cardiff.ac.uk

tions, pre-impinging spray characteristics, and impact angle, and also surface characteristics such as geometrical shape, temperature and roughness. The characterisation of post-impingement spray is often performed using Phase Doppler Anemometry (PDA) (e.g. [6], [9], and [10]), since this technique offers considerable potential for quantification of post-impact droplet sizes and flowfield. However, a full understanding of the spray impact process requires characterisation of any residual fuel film. Hence, time-resolved spatial field measurements of droplet size need to be complemented by characterisation of the resulting liquid film on the wall.

This paper describes the potential of TIR-LIF, proposed by Alonso et al [1], for characterisation of transient liquid fuel films formed as a result of spray impingement, which provides a tool for validation of spray impact models when used in conjunction with PDA. This technique is an extension of LIF in which the propagation of a laser beam is carefully controlled so as to target the excitation of the liquid fuel film only and not the airborne droplets above the film. Calibrated benchmark results reported by the authors demonstrate the ability of this technique for spatial and temporal characterisation of fuel films throughout the injection event. Quantitative results reported include time resolved two-dimensional distribution maps of fuel film thickness, aggregates of total mass deposits, and mean and maximum film thickness. An analysis of fuel films for multiple injections is presented in this paper to demonstrate the applicability of this technique for analysis of fuel films with dry and wet pre-impingement walls. Results obtained by TIR-LIF, in conjunction with post-impingement PDA characterisation, can be used for appraisal of current spray impact models, and for development of new post-impingement empirical models to describe this phenomenon.

Experimental set-up

The TIR-LIF technique is based on the principle that upon excitation by laser light, the intensity of the fluorescent signal from a tracer is proportional to the film thickness. The principle of the TIR-LIF technique is described in detail by Alonso et al [1], and will not be reported here again. Nevertheless, it is worthwhile summarising that the critical angle to ensure total internal reflection, calculated for the same optical setup, is 43.81°. For this experimental setup, the maximum angle to ensure transmittance in the quartz-fuel interface is 69°, and the optimum angle of incidence found at 65°, which is the angle utilised throughout this experiment. Figure 1 shows a schematic of the TIR-LIF optical set-up used for characterisation of fuel films. Based on the principle of total internal reflection, the propagation of the exciting laser beam is controlled to target the fuel film. The optical piston was specifically designed so that the beam is directed towards the top surface at the desired angle, an angle that allows transmittance to the liquid fuel film and ensures total internal reflection to avoid excitation of airborne fuel.

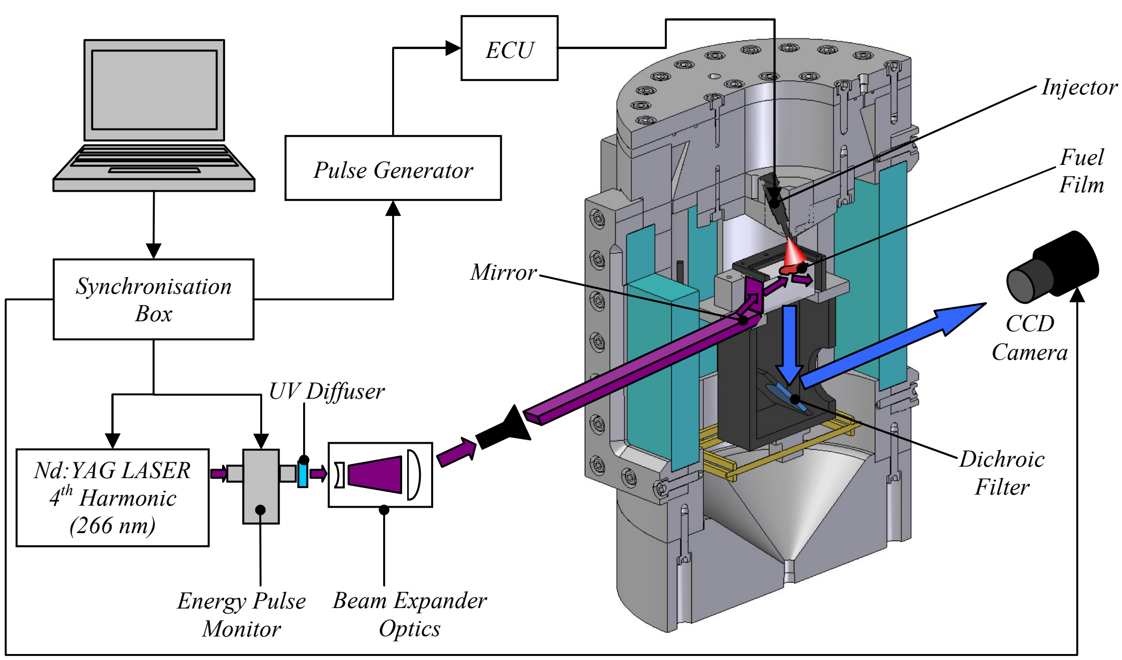

Figure 1. Experimental setup for impingement experiments at elevated ambient pressures

The rig allows independent accurate control of ambient pressures and ambient temperatures of up to 1.5 MPa and 423 K respectively. In order to increase the size of the interrogation area, the nominal beam diameter of 8 mm is expanded to 40 mm using a plano-concave singlet lens (Melles Griot: 01 LQP 003) and a plano-convex singlet lens (Melles Griot: 01LQP027). This allows the illumination of a large area, big enough to accommodate the whole fuel film at once (approximately 40 x 40 mm). A binary mixture of 10 % 3-Pentanone in Isooctane is used as a substitute of gasoline due to its similar thermofluid properties [11]. A frequency quadrupled Nd:YAG laser at wavelength 266 nm is used as the excitation light source and an intensified CCD camera records the results as fluorescent images. The images are acquired from several cycles and phase averaged in order to build a full map of the transient fuel film. The fluorescence signal is acquired through a 50mm Nikkor Lens (f/1:4) onto a Hamamatsu gated image intensifier linked to a Hamamatsu HiSense Mk II CCD camera with a resolution of 1344 x 1024 pixels. The fluorescent signal of 3-pentanone, when excited at 266 nm, peaks around 400 nm [11]. Therefore, a 400 nm short band pass filter (Schott BG4 glass) is used to optimise the fluorescence signal from the excited fuel film. This filter offers > 90 % transmission in the peak fluorescence, while blocking any possible scattered light of the laser at 266 and 532 nm. In addition, specially coated mirrors are used to maximise the transmittance of both laser the excitation light (266 nm), and the fluorescence signals (400 nm). An Energy Pulse Monitor (EPM) is used to account for laser power fluctuations (shot-to-shot variation) in the calibration process, as this device allows instantaneous laser power measurements. A 5º full width half maximum (FWHM) UV diffuser optic is used to attenuate the typically uneven power distribution of the Nd:Yag laser beam pattern, making the beam profile more homogeneous (‘top-hat shape’).

Alonso et al [1] demonstrated that the intensity of fluorescence emitted by 3-pentanone excited at 266 nm is linearly proportional to the product of the thickness and concentration of the tracer for a ‘thin’ film layer of a homogeneous mixture. For the application of LIF to fuel films measurements, it is possible to determine the ratio between fluorescence and film thickness when the volume, footprint area, and intensity distribution of a fuel film are known. In order to calibrate the fluorescence for the current experimental set-up, images of known volumes of liquid fuel films are placed on the measurement surface by means of a micro-syringe to obtain calibration images. The fluorescent signal of various volumes from 10 to 50 micro-litres was acquired to build the calibrations curve, which is presented in figure 2d.

In order to obtain quantitative information from TIR-LIF studies, the raw images need to be carefully post-processed. This paper uses the same post-processing methodology described by Alonso et al [1], also used by Seitzman and Hanson [12] and Zhao and Landommatos [13]. The image calibration sequence is presented in figure 2. The first step involves the removal of systematic errors present in the imaging system. Therefore, a background image combining the background and dark current signals is subtracted from the recorded raw image. This image is obtained by removing the fluorescent particles from the system. An average background image is preferred to minimise the effect of shot-to-shot variation.

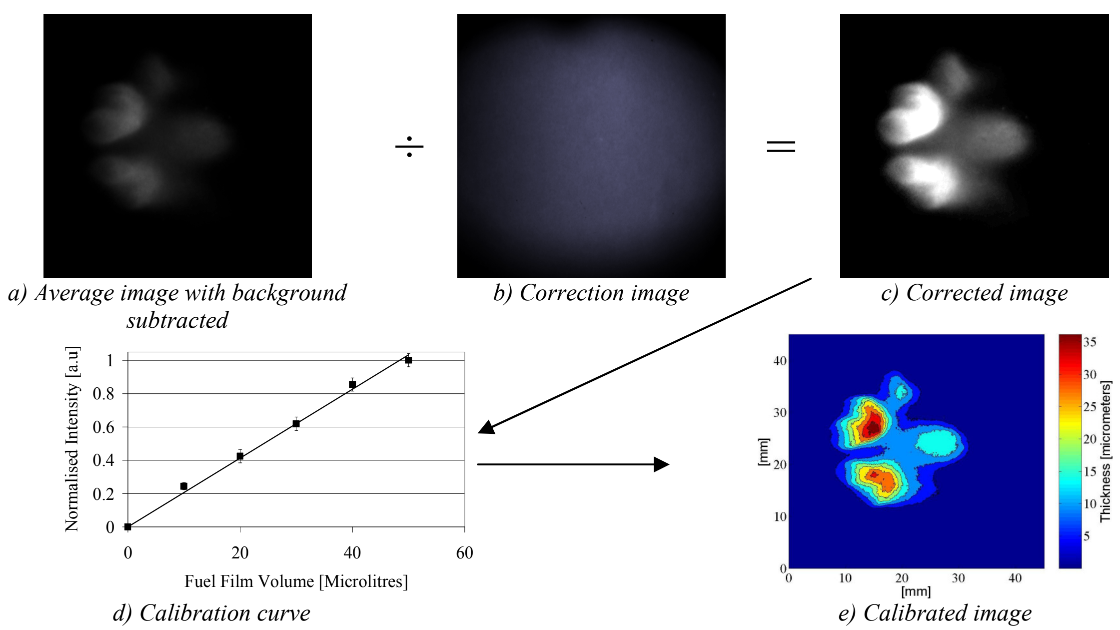

Figure 2. Image Processing sequence. TIR-LIF image for time = 1.75 ms ASOI and P_a = 0.1 MPa

Figure 2a shows an average of 20 images resulting from subtracting each raw image from the background image. Subsequently, the resulting image is divided by a correction image (figure 2b) to account for spatial variations in the responsivity of the detector, and non-uniformities of the laser sheet. The correction image is obtained from a homogeneous mixture containing fluorescent particles minus the background image. The corrected image of the fluorescent signal, figure 2c, can be calibrated using the calibration curve for its corresponding ambient conditions (figure 2d). Finally, the method produces a calibrated image of the liquid film, figure 2e, where both the thickness and footprint dimensions can be obtained across the impingement plane.

Results and Discussion

Transient fuel film deposits of an impinging gasoline DI spray, investigated using the TIR-LIF method, are discussed in this section. Quantitative results of fuel impingement under atmospheric ambient pressure (0.1 MPa) are presented for an impinging spray from a Bosch C2-70 pressure swirl injector located 21 mm from the surface and angled at 45º with respect to the normal of the impact plane. The experimental fuel line pressure is 10 MPa, and the injection duration 1.5 ms. The tests is conducted at a constant ambient temperature of 295 K.

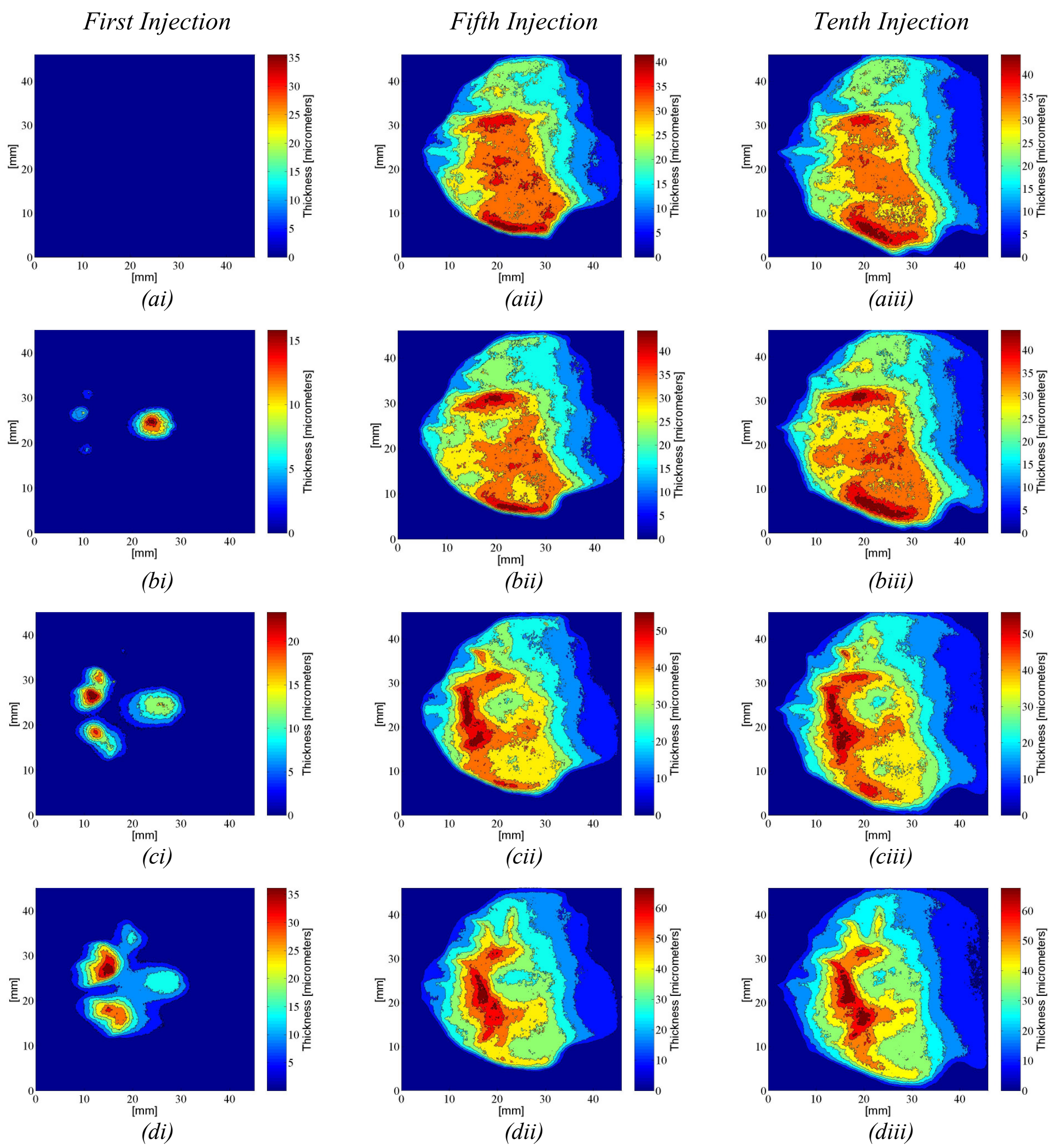

Figure 3. Transient fuel thickness measurements for multiple injections for selected times ASOI: (a) 1.00 ms, (b) 1.25 ms, (c) 1.50 ms, (d) 1.75 ms.

An analysis of fuel films for multiple injections is presented in this section to demonstrate the applicability of this technique for analysis of fuel films with dry and wet pre-impingement walls. In the calibrated images, e.g. figure 2e, the pre-impinging spray propagates from left to right and the tip of the injector is located in the centre of the left side of the images (at y = 22.5 mm). Figure 3 shows transient fuel thickness measurements for multiple injections for selected times after start of injection: (a) 1.00 ms, (b) 1.25 ms, (c) 1.50 ms, and (d) 1.75 ms. The column on the left (column i) illustrates the development of the fuel film for a single injection with dry pre-impingement conditions. The column in the centre (column ii) and the column of the right (column iii) describe the development of the fuel film for the fifth and tenth injection respectively, with wet pre-impingement conditions due to deposits from four and nine previous injections separated by 200 milliseconds.

For the first timebin, at 1.00 ms ASOI, the spray has not reached the measurement plane as can be seen in figure 3ai. Since the spray from the current injection has not reached the measurement plane for this timebin, the fuel film from previous injections has sufficient time (200 milliseconds) to stabilise and re-distribute across the impingement plane. Consequently, the pre-impingement wet wall shown in figure 3aii and 3aiii illustrates a relatively uniform thickness of 25 microns with most of the deposits located in the bottom of the image (due to the rotational component of the spray). At 1.25 ms ASOI, the sac volume and the bottom half of the hollow cone can be identified for the first injection (figure 3bi), while the sac volume can also be vaguely identified on the fifth and tenth injection as a small hole (thinner region) in the centre of the image (figures 3bii and 3biii). For the following timebin, 1.50 ms ASOI, figures 3cii and 3ciii show clearly a 'crater' structure in the centre of the image produced as a result of displacement of mass within the film due to impact of the sac volume with high inertia. Additionally, a 'crescent moon' shape region with higher thickness can be identified in both images to the left of the crater which describes a large accumulation of fuel in the cone impact region. Subsequent timebins describe the development of a surface wave as a result of the elevated deposits during the cone impact as can be seen in the sequence of images 3cii, and 3dii (or 3ciii and 3diii for the tenth injection). During this time, from 1.50 to 1.75 ms ASOI, there is continuous deposition of fuel on the surface, which applies momentum to the small wave front forcing it to propagate across the impingement plane. After 2.25 ms, all the pre-impact spray reaches the surfaces marking the end of the deposition phase, for which no more momentum is applied to the wave front. Therefore, after this time, the surface wave propagates across the film for a short period, loosing momentum, until it tends to die-out creating a relatively uniform film distribution. Eventually, after sufficient time, they produce a film similar to that on figure 3aii, which marks the boundary condition for the next injection.

A time resolved fuel film thickness plot for multiple injections is presented in figure 4. The average and maximum thickness of 10 consecutive injections (separated by 200 milliseconds) are superimposed in this figure to illustrate the development of the fuel film. The average thickness is calculated by integrating values of thickness across the impingement plane. Figure 4a shows the average thickness of the fuel film, where a good agreement is observed in successive injections. For instance, a similar average thickness is observed in the latter stages of the first injection and the early timebins of the second injection prior to the impact of fuel, and so on. In general, a small reduction of thickness from the final deposits of a particular injection is observed in early stages of the following injection due to evaporation of the fuel during the 200 milliseconds gap between injections.

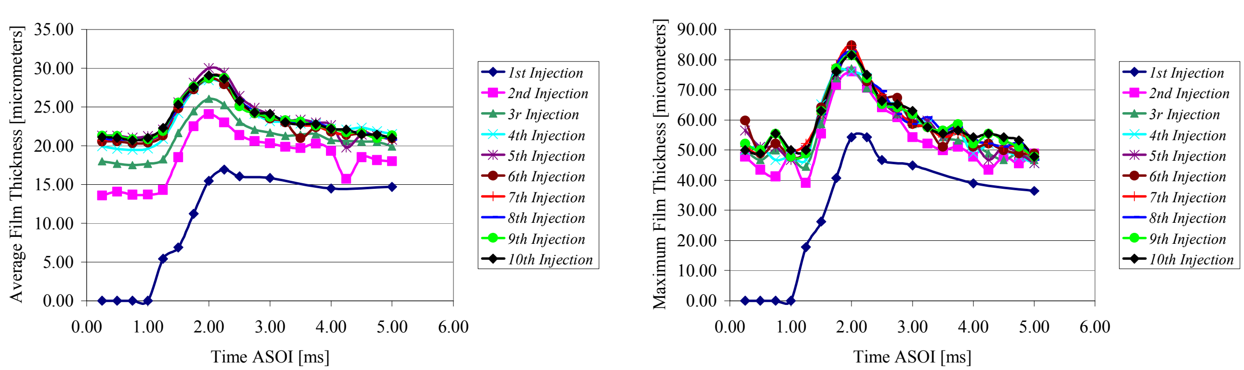

(a) (b)

Figure 4. Average (a) and Maximum (b) Thickness for multiple injections.

Between 0.25 and 1.00 ms ASOI, the average thickness measured for all injections is constant because the spray has not reached the impact surface, and the measurements correspond to the film from previous injections. After this time, between 1.25 and 2.25 ms ASOI, there is continuous deposition of fuel on the surface which is observed in figure 4a as a sharp increase in the film thickness. The first injection shows a slow decay after 2.25 ms as the film is redistributed across the impingement plane. The rest of injections (from 2nd to 10th) reach a maximum at 2.25 ms ASOI, after which a significant decrease in average film thickness is observed. This maximum is attributed to the high localised fuel film thickness observed on the wave front described in figure 3, which loses inertia after 2.25 ms and tends stabilise the film thickness for further timebins. Figure 4a shows that the fuel film reaches a saturation point at the fourth injection, after which the average thickness is very similar for subsequent injections. This saturation is only observed for the thickness component, since the liquid film continues increasing its size and mass in later injections, implying further deposits for subsequent injections. After the 4th injection, the average thickness of the pre-impingement wet wall is approximately 20 microns, which is slightly larger than the global SMD of the pre-impacting spray (approx. 18 microns). The relative high thickness of the wet wall in comparison with the pre-impact droplet diameters is thought to be the primary cause for the thickness saturation of the liquid film. However, this, along with other potential explanations, would require further experimental study and analysis to be fully confident of the underlying causes. A maximum fuel film thickness plot is presented in figure 4b, which shows a similar trend for early timebins to that discussed for 4a (before 2.25 ms). However, after 2.25ms, a sharper decay is observed for all the injections as wave front dies out levelling the thickness across the liquid film.

Conclusions

This paper described the use of TIR-LIF for characterisation of transient liquid fuel films formed as a result of impingement of a gasoline DI spray on a flat surface. The technique proved successful at characterising, qualitatively and quantitatively, the development of fuel films for multiple injections, particularly describing the transient effect of the fuel film thickness and shape. Analysis of multiple injections separated by 200 milliseconds explored the potential of the technique for chararacterisation of liquid films with dry and wet pre-impact walls. After the 4th injection, an average fuel thickness or approx. 20 microns is observed. After this injection, the liquid film thickness saturates, favoring an increase in footprint size to accommodate deposits from subsequent injections. Results obtained by TIR-LIF, when used in conjunction with post-impingement PDA characterisation, demonstrate considerable potential for appraisal of current spray impact models, and for development of new post-impingement empirical models to describe this phenomenon. Future work will explore the potential of the technique for tests at elevated ambient pressure and temperature. Also, a simpler experimental setup will be considered to for a full analysis of spray-impact models exploring the possibility for sub-model improvements.

References

1. Alonso M., Kay P.J., Bowen P.J., Gilchrist R., and Sapsford S.: Quantification of 3D Transient Fuel Films for G-DI Sprays Under Elevated Ambient Conditions, *22nd European Conference on Liquid Atomization and Spray Systems*, Como Lake, Italy, 8-10 September, (2008).
2. Cossali G.E., Marengo M., and Santini M., *Atomisation and Sprays*, 15:699-736 (2005).
3. Bai C., and Gosman A..D., *Society Automot. Eng*, 950283:69–87 (1995)
4. Mundo C., Sommerfeld M., Tropea C., *Atomization and Sprays*, 8: 625–652 (1998)
5. Stanton D.V., and Rutland C.J., *Int. J. Heat Mass. Transfer*, 41:3037–3054 (1998)
6. Kalantari D., and Tropea C., *Int. J. Multiphase Flow*, 33:525-544 (2007)
7. Cossali G.E., and Coghe A., and Marengo M., *Experiments in Fluids*, 22:463–472 (1997)
8. Sivakumar S., and Tropea C., *Phys. Fluids Lett.*, 14L:85–88 (2002)
9. Panao M.R.O., and Moreira A.L.N., *Proceedings of the Combustion Institute*, 31:2205-2213 (2007)
10. Cossali G.E., Marengo M., and Santini M., *International Journal of Heat and Fluid Flow*, 29: 167-177 (2007)
11. Schulz C., and Sick V., *Prog Energy Combust Sci.*, 31:75-12 (2005)
12. Seitzman J.M., Hanson R.K. *Instrumentation for flows with combustion*. A.M.K.P. Taylor. Academic Press, 1993, pp 405-466.
13. Zhao H., and Ladommatos N., *Prog Energy Combust Sci.*, 24: 297-336 (1998)